SAND2022-14186C

Sandia National Laboratories

Magnetized Liner Inertial Fusion (MagLIF): Developing a data-driven understanding of magnetic flux compression from computation through experiment

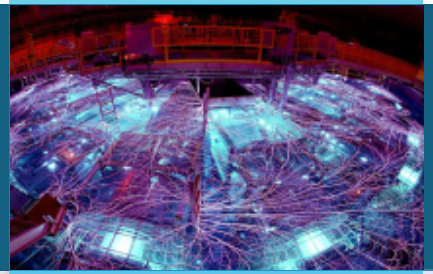

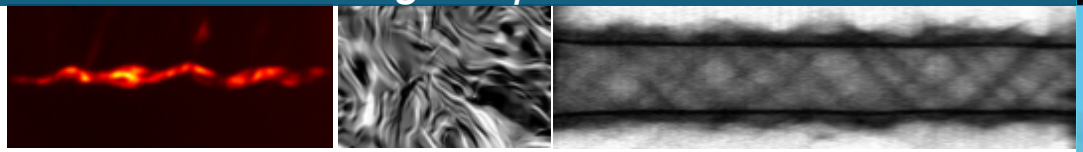

PRESENTED BY

William Lewis

APS DPP
10/20/22

P.F. Knapp, S.A. Slutz, P.F. Schmit*, G.A. Chandler, M.R. Gomez, A.J. Harvey-Thompson, M.A. Mangan, D.J. Ampleford, and K. Beckwith

For new results that will be presented, **special thanks** to O.M. Mannion, C.A. Jennings, D.E. Ruiz,
P.F. Knapp, M.R. Gomez, and A.J. Harvey-Thompson

SAND2022-#### C

We are applying modern data-driven methods to accelerate the design and discovery cycle at Sandia's Z pulsed power facility.

Optimization of Diagnostic Configurations in the Presence of Uncertainty Using Bayesian Inference and Optimization

P. Knapp *et al.* **GO06.00005** on 10/17/22

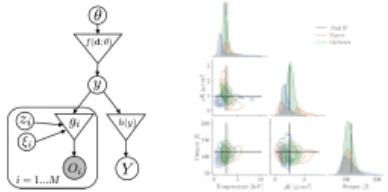

P.F. Knapp *et al.* J. Plasma Phys. (Under review).

Identifying Governing ODEs in Irregular Physical Domain with Diffusion

G. Vasey *et al.* **NP11.00069** on 10/19/22

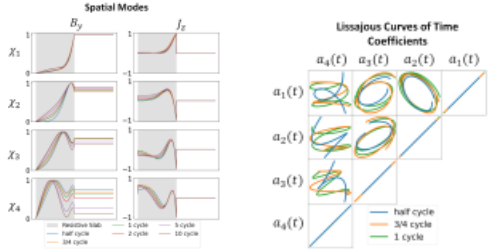

Bayesian Analysis Applied to Neutron Activation Diagnostics Measurements of MagLIF

M. Mangan *et al.* **TP11.00084** on 10/20/22

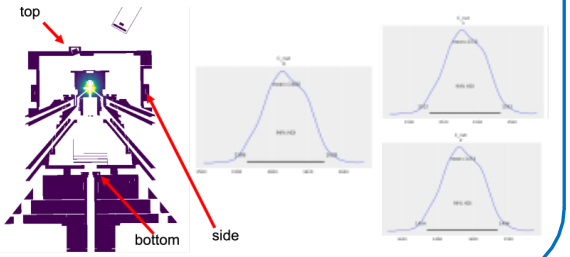

An autoencoder based reduced order model of low density plasma for optimal experimental design

R. Patel *et al.* **CO05.00011** on 10/17/22

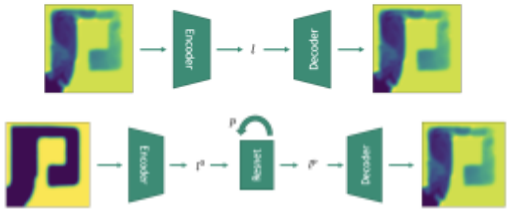

Analysis of the scattered neutron energy spectrum from magnetized liner inertial fusion implosions on Z

O. Mannion *et al.* **NO04.00007** on 10/19/22

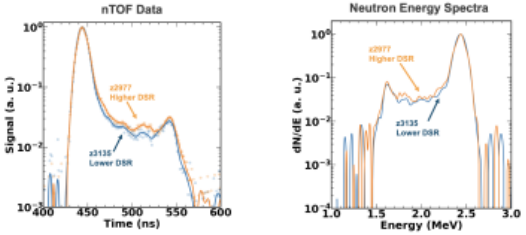

Quantifying data constraints for velocimetry-based load current determination for inertial confinement fusion targets

A. Porwitzky *et al.* **YO04.00006** on 10/21/22

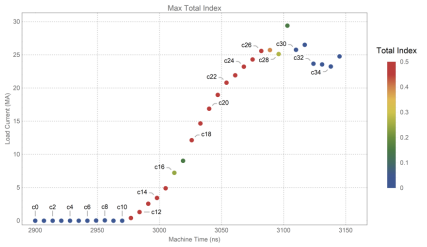

We are applying modern data-driven methods to accelerate the design and discovery cycle at Sandia's Z pulsed power facility.

This talk W.E. Lewis *et al.,* Phys. Plasmas (2021). Selected as an Editor's Pick

- **Assessment of fuel magnetization in MagLIF**
  - First-ever systematic study of magnetic confinement properties of any neutron producing magneto-inertial fusion platform
    - Enabled by deep-learning and Bayesian inference
    - Experimental evidence for the role of Nernst advection in flux loss

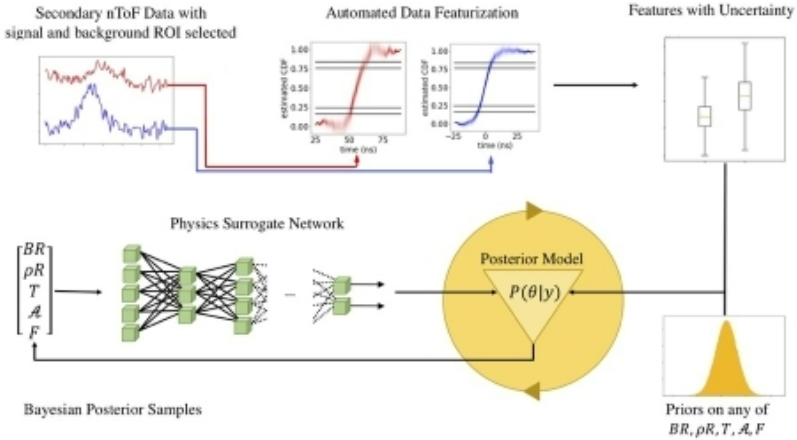

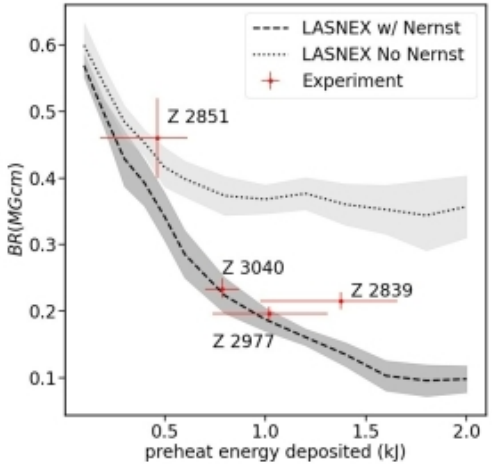

W.E. Lewis *et al.,* Phys. Plasmas **28**, 092701 (2021).

We are applying modern data-driven methods to accelerate the design and discovery cycle at Sandia's Z pulsed power facility.

This talk W.E. Lewis *et al.,* Phys. Plasmas (2021). Selected as an Editor's Pick

How does changing other experimental inputs impact flux loss?

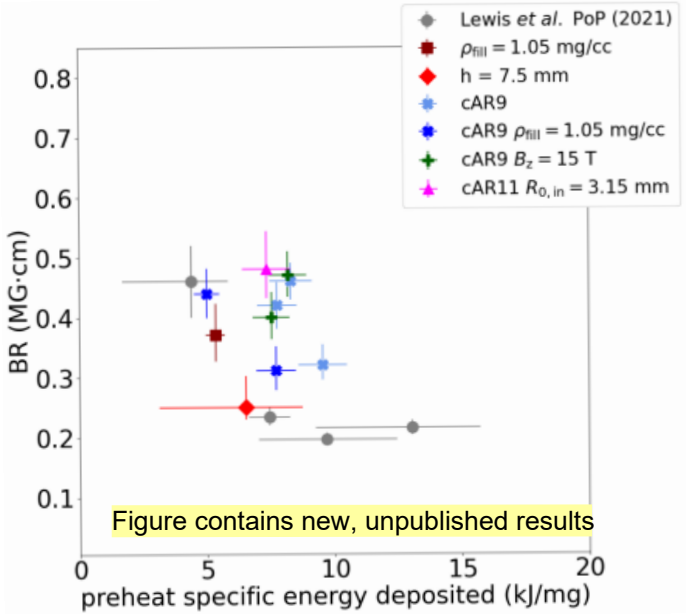

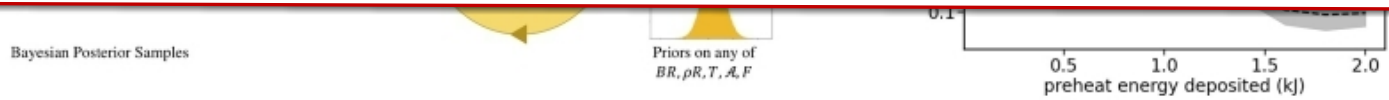

W.E. Lewis *et al.,* Phys. Plasmas **28**, 092701 (2021).

MagLIF relies on three stages to reach fusion relevant conditions.

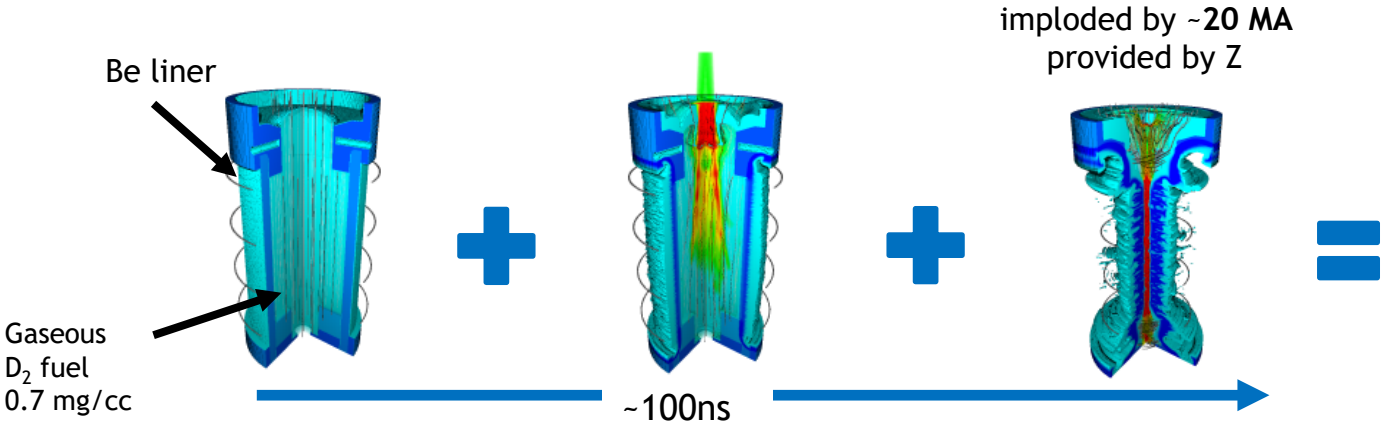

Apply Axial Magnetic Field

- Suppress radial thermal conduction losses

Preheat

- Increase fuel adiabat to limit required convergence
- Ionize fuel to lock in B-field

Implosion

- PdV work to heat fuel
- Amplify B-field through flux compression
  - critical for confining 3.5 MeV alphas
  - For pure-D fuel, it also confines 1.01 MeV DD tritons, which enhances secondary DT reactions

Stagnation

- Several keV temperatures
- Several kT B-field to trap charged fusion products

S.A. Slutz *et. al.*, PoP (2010)

MagLIF relies on three stages to reach fusion relevant conditions.

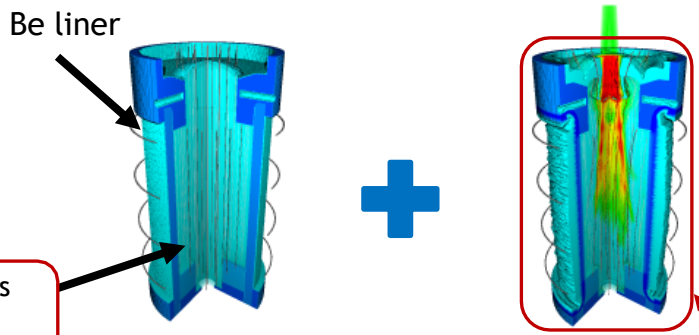

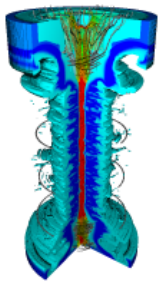

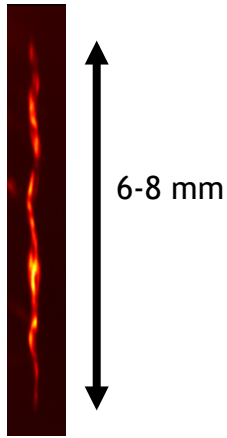

~100ns

Apply Axial Magnetic Field **Preheat** **Implosion** **Stagnation**

Developing solid cryogenic fuel configurations for magnetic direct drive inertial confinement fusion targets

T. Awe *et al.* **QI02.00002** up next

Advances in hybrid-CMOS X-ray framing cameras for High-Energy-Density science research

J. Porter **QI02.00004** last in this session

S.A. Slutz *et. al.*, PoP (2010)

Magnetization, or magnetic field-fuel radius product (BR), is a critical confinement parameter for MagLIF.

Effective BR for $B_z(r)$ profile:

$$\overline{BR} = \frac{\Phi_R}{\pi R} = \frac{2}{R}\int_0^R rB_z(r)dr$$

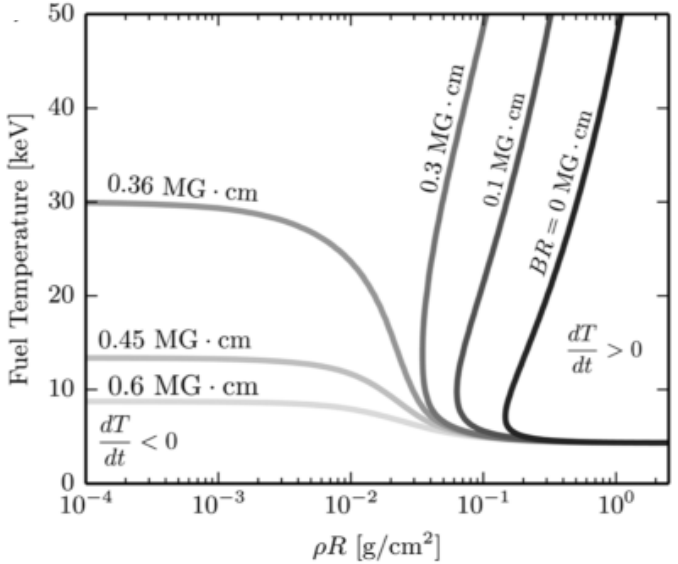

P.F. Knapp *et. al.*, PoP (2015)

$\overline{BR}$ determines trapping of fast charged particles:

trapping condition for particles born at r=0 $\overline{BR} \geq \sqrt{\frac{8mE_\perp}{q^2}}$

A variety of plasma transport effects will modify the flux compression process. Measuring BR could provide insights into these effects.

- Ideal flux compression ~1000x B-field amplification
  - trapping of fusion products and reduction of electron heat conduction
- Physical mechanisms leading to flux loss
  - Resistive diffusion
  - Nernst

$$v_{Nernst} = \frac{\beta_\wedge \nabla_\perp T_e}{eB}$$

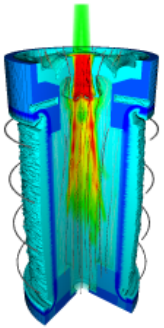

Resistive diffusion

- Current disrupted by collisions
  - Allows magnetic field diffusion

$$\sim \quad 0 \quad 2$$

$$\propto$$

Nernst effect

- B-field locked into warm electrons
- Thermal transport perpendicular to B transports flux

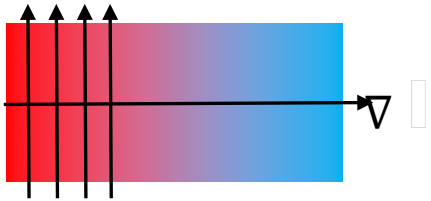

- Increased preheat $\propto \nabla_\perp T_e$ increases Nernst
- Increased B_z decreases Nernst
- What about geometry?
- Fill density?
- Impact of mix throughout implosion
- Measurements needed to study effects
  - **can't do proton deflectometry/radiography**
    - **O(50 MG) fields driving Z-pinch!**

S. Malko *et al.* **TO06.00009** on 10/20/22
"**Detailed benchmarking of the Nernst effect in magnetized HED plasma**"

Radially and axially viewed secondary DT neutron spectra and yield ratio $\bar{Y} = Y_{DT}/Y_{DD}$ are sensitive to fuel magnetization.

- Pure Deuterium fuel
  - ~1.01 MeV tritons produced by DD fusion

$$\text{Primary:} \quad D + D \rightarrow \begin{cases} n\ (2.45\text{MeV}) + {}^3He \\ p + T\ (1.01\text{MeV}) \end{cases}$$

$$\text{Secondary:} \quad D + T \rightarrow n\ (14.1\text{MeV}) + \alpha$$

$$\mathcal{P}_{DT} \propto \langle \rho_D \ell \rangle \sigma_{DT} \xrightarrow{\text{Magnetized}} \ell \propto \left(\quad \right)$$

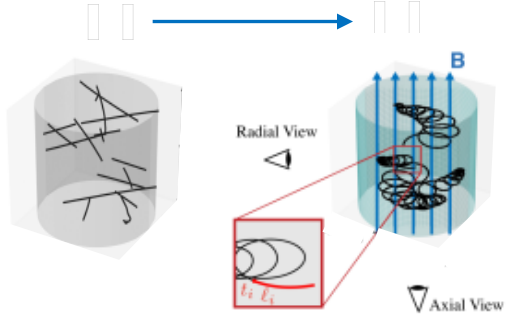

P.F. Schmit *et al.*, PRL (2014)
P.F. Knapp *et. al.*, PoP (2015)

- Surrogacy of tritons for $\alpha's$
  - similar Larmor radius
  - 3.5 MeV α stopping length ~ 0.5x1.01 MeV tritons

Increase in P_{DT} increases $\bar{Y}$

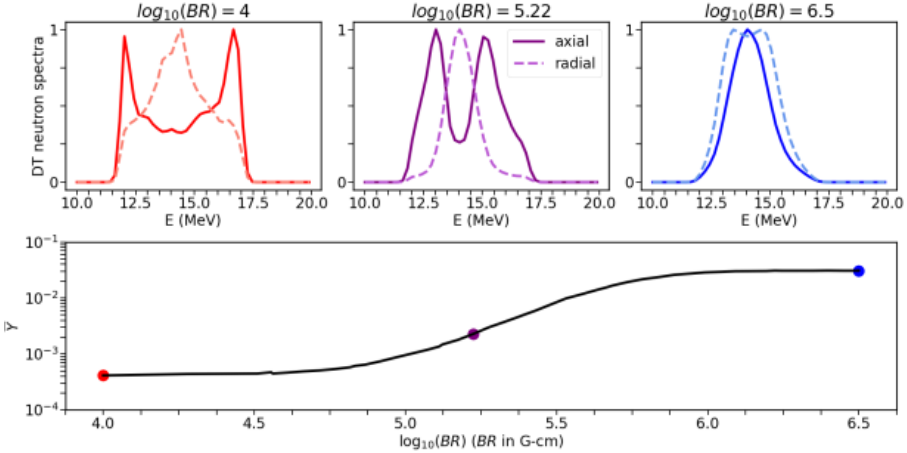

W.E. Lewis *et al.,* Phys. Plasmas **28**, 092701 (2021)

Radially and axially viewed secondary DT neutron spectra and yield ratio $\bar{Y} = Y_{DT}/Y_{DD}$ are sensitive to fuel magnetization.

- Pure Deuterium fuel
  - ~1.01 MeV tritons produced by DD fusion

$$\text{Primary:} \quad D + D \rightarrow \begin{cases} n\ (2.45\text{MeV}) + {}^3He \\ p + T\ (1.01\text{MeV}) \end{cases}$$

$$\text{Secondary:} \quad D + T \rightarrow n\ (14.1\text{MeV}) + \alpha$$

$$\mathcal{P}_{DT} \propto \langle \rho_D \ell \rangle \sigma_{DT} \xrightarrow{\text{Magnetized}} \ell \propto \ (\ \ )$$

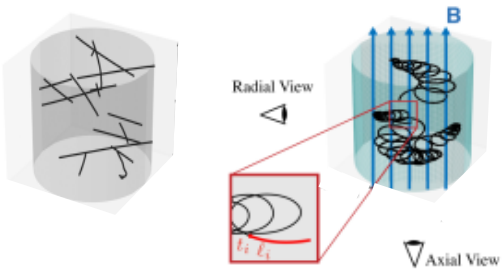

P.F. Schmit *et al.*, PRL (2014)
P.F. Knapp *et. al.*, PoP (2015)

- Surrogacy of tritons for $\alpha's$
  - similar Larmor radius
  - 3.5 MeV α stopping length ~ 0.5x1.01 MeV tritons

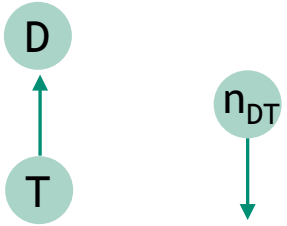

14 MeV in CM
Doppler down shift

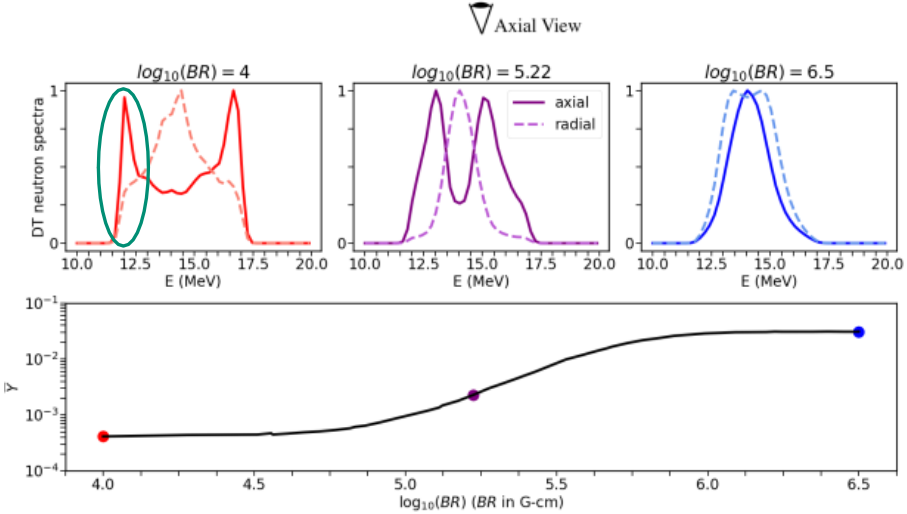

W.E. Lewis *et al.,* Phys. Plasmas **28**, 092701 (2021)

Radially and axially viewed secondary DT neutron spectra and yield ratio $\bar{Y} = Y_{DT}/Y_{DD}$ are sensitive to fuel magnetization.

- Pure Deuterium fuel
  - ~1.01 MeV tritons produced by DD fusion

$$\text{Primary:} \quad D + D \rightarrow \begin{cases} n\ (2.45\text{MeV}) + {}^3He \\ p + T\ (1.01\text{MeV}) \end{cases}$$

$$\text{Secondary:} \quad D + T \rightarrow n\ (14.1\text{MeV}) + \alpha$$

$$\mathcal{P}_{DT} \propto \langle \rho_D \ell \rangle \sigma_{DT} \xrightarrow{\text{Magnetized}} \ell \propto \ (\ \ )$$

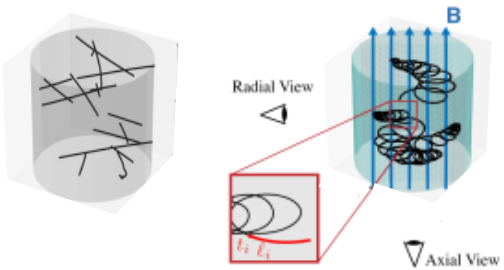

P.F. Schmit *et al.*, PRL (2014)
P.F. Knapp *et. al.*, PoP (2015)

- Surrogacy of tritons for $\alpha's$
  - similar Larmor radius
  - 3.5 MeV α stopping length ~ 0.5x1.01 MeV tritons

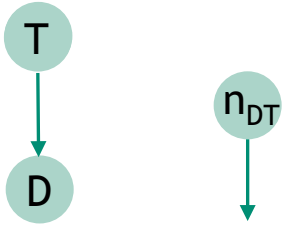

14 MeV in CM
Doppler up shift

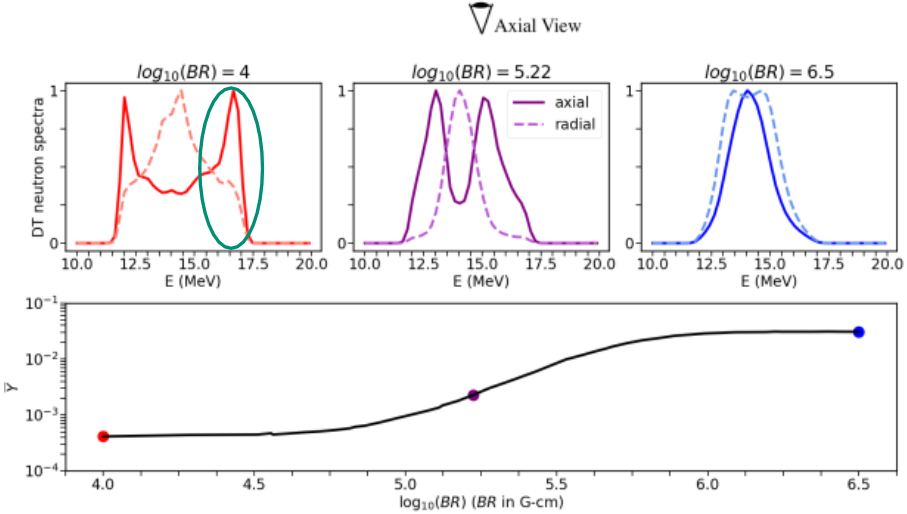

W.E. Lewis *et al.,* Phys. Plasmas **28**, 092701 (2021)

Radially and axially viewed secondary DT neutron spectra and yield ratio $\bar{Y} = Y_{DT}/Y_{DD}$ are sensitive to fuel magnetization.

- Pure Deuterium fuel
  - ~1.01 MeV tritons produced by DD fusion

$$\text{Primary:} \quad D + D \rightarrow \begin{cases} n\ (2.45\text{MeV}) + {}^3He \\ p + T\ (1.01\text{MeV}) \end{cases}$$

$$\text{Secondary:} \quad D + T \rightarrow n\ (14.1\text{MeV}) + \alpha$$

$$\mathcal{P}_{DT} \propto \langle \rho_D \ell \rangle \sigma_{DT} \xrightarrow{\text{Magnetized}} \ell \propto \ (\ \ )$$

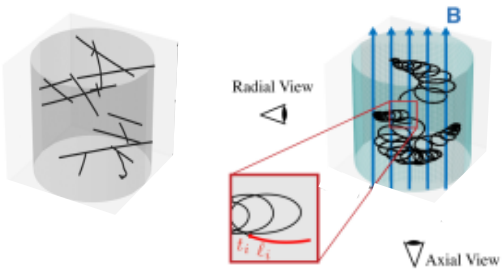

P.F. Schmit *et al.*, PRL (2014)
P.F. Knapp *et. al.*, PoP (2015)

- Surrogacy of tritons for $\alpha's$
  - similar Larmor radius
  - 3.5 MeV α stopping length ~ 0.5x1.01 MeV tritons

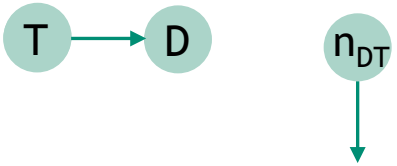

14 MeV in CM
No Doppler shift
B_z ~ probability

Low probability

Axial View

High probability

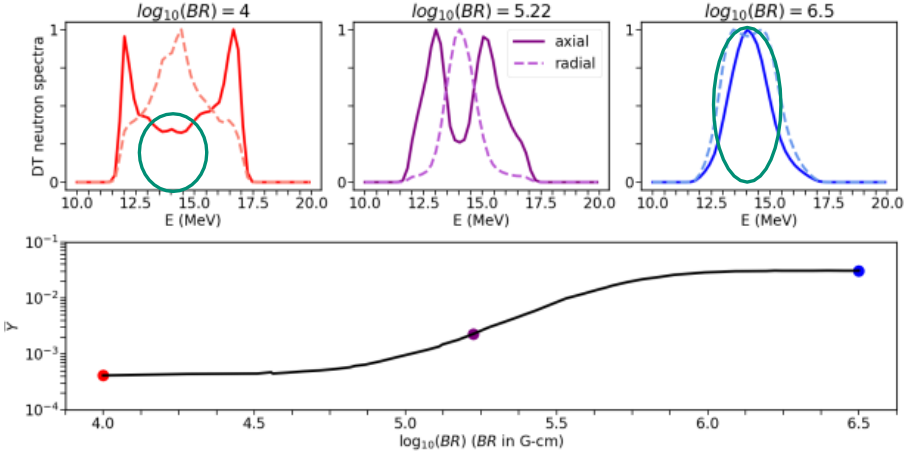

W.E. Lewis *et al.,* Phys. Plasmas **28**, 092701 (2021)

Our analysis is based on a Bayesian inference which makes use of NN surrogate for speedup of physics model.

Obtain secondary neutron Time of Flight (nToFs)

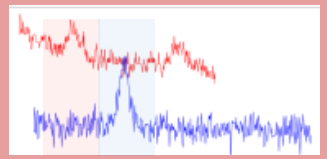

Select ROIs

Provide DT and DD yields with uncertainty

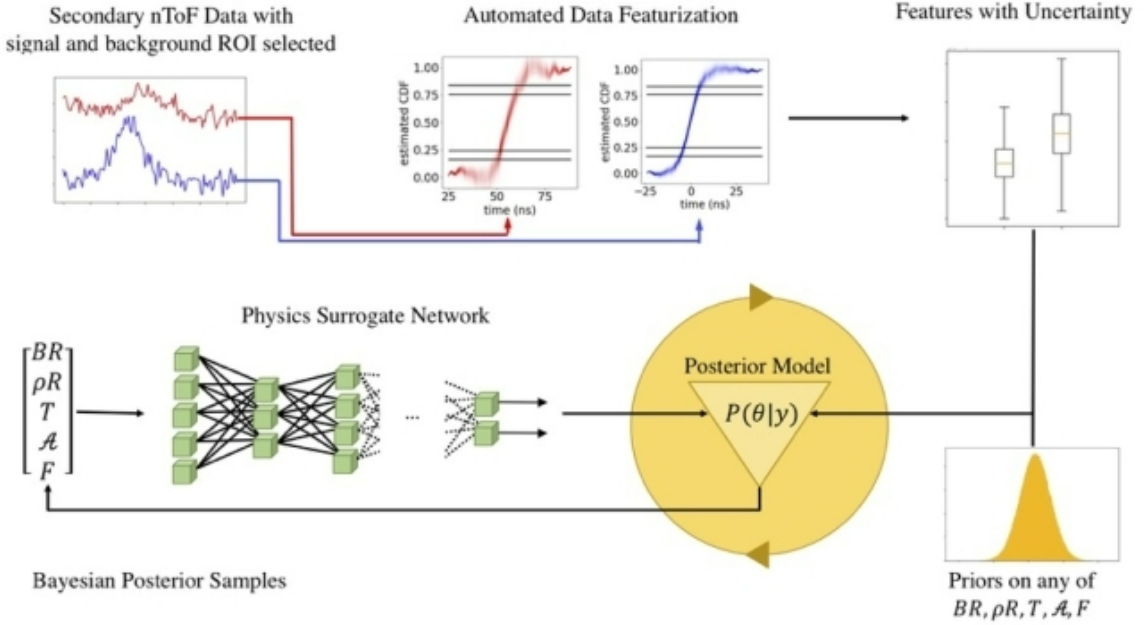

W.E. Lewis *et al.,* Phys. Plasmas **28**, 092701 (2021).

Our analysis is based on a Bayesian inference which makes use of NN surrogate for speedup of physics model.

Obtain secondary neutron Time of Flight (nToFs)

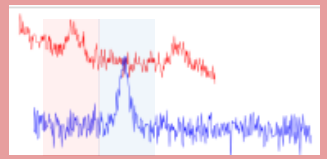

Select ROIs

Provide DT and DD yields with uncertainty

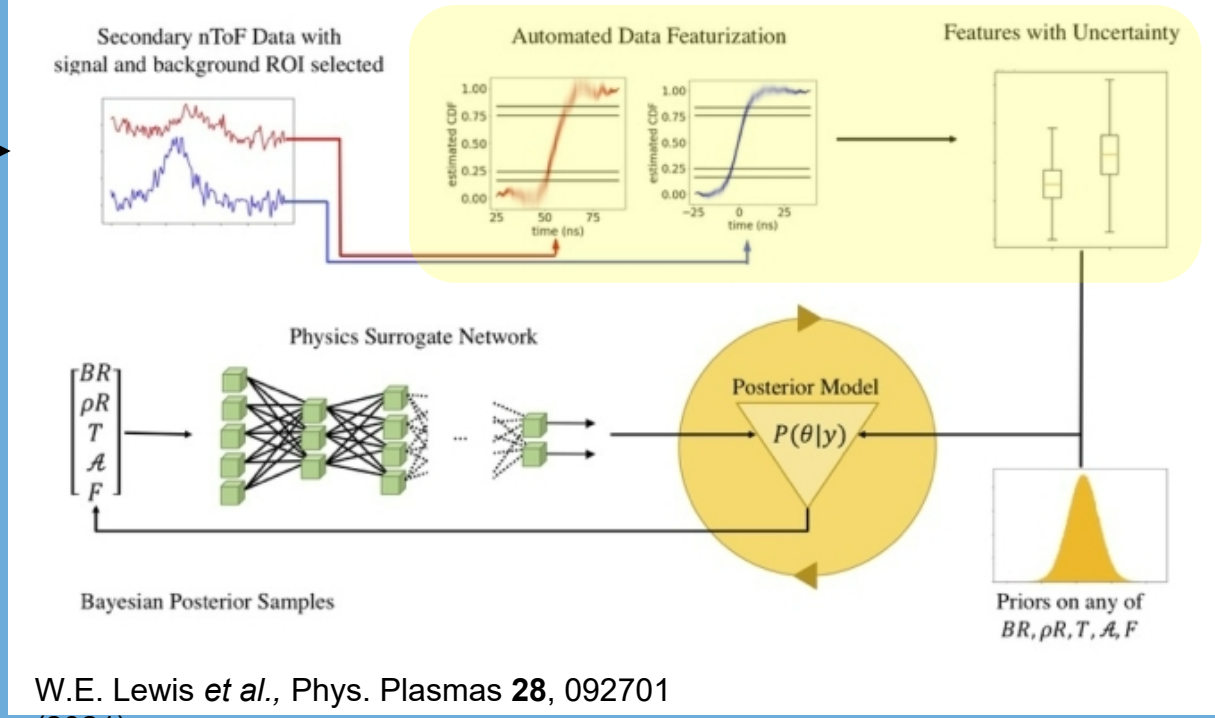

W.E. Lewis *et al.,* Phys. Plasmas **28**, 092701 (2021).

We wish to “featurize” the nToF data collected experimentally to reduce dimensionality while retaining relevant information.

- Width and asymmetry features with uncertainty
  - percentiles of nToF signals
    - integration smooths noise
    - error from Bayesian fitting
- nToF avoids *e.g.*
  - unavailable timing fiducial
  - ill-posed instrument response deconvolution

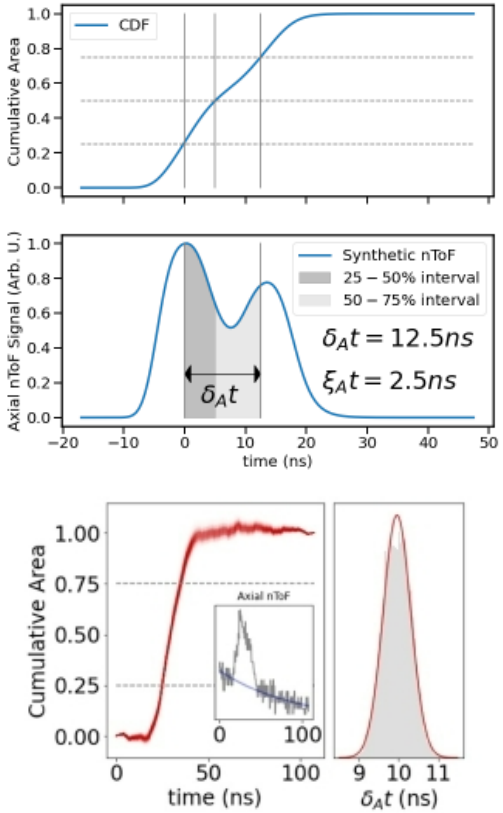

W.E. Lewis *et al.,* Phys. Plasmas **28**, 092701

Our analysis is based on a Bayesian inference which makes use of NN surrogate for speedup of physics model.

Obtain secondary neutron Time of Flight (nToFs)

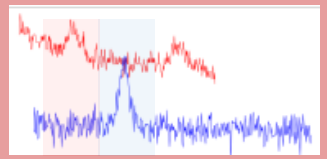

Select ROIs

Provide DT and DD yields with uncertainty

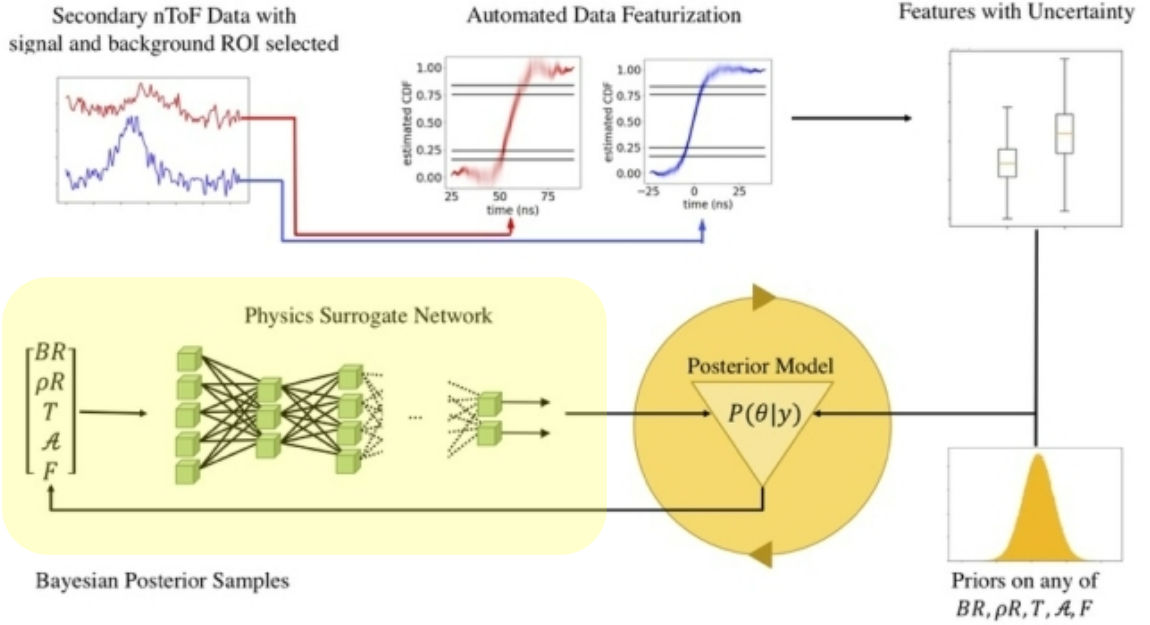

W.E. Lewis *et al.,* Phys. Plasmas **28**, 092701 (2021).

Costly analysis results in the need for data-driven approaches to routinely invert experimental data for BR.

- Previously, one experiment analyzed for BR in the literature:
  - P.F. Schmit *et al.*, Phys. Rev. Lett. (2014)
  - P.F. Knapp *et. al.*, Phys. Plasmas (2015)
- Computational cost of forward physics model
  - O(10-100) CPU hours evaluation on a high-performance cluster
  - 10k-100k + evaluations per experiment for inference and uncertainty quantification
- Use a **surrogate model/fast emulator**
  - Rigorous UQ with **Bayesian statistics** feasible with

neural network surrogate, which drastically improves evaluation times.

- ~65k simulation samples
  - 95%-4%-1% train-validation-test split
- neural network with skip connections
  - about 5.5k fit parameters
- Validation data used to estimate error
  - propagate uncertainty of surrogate

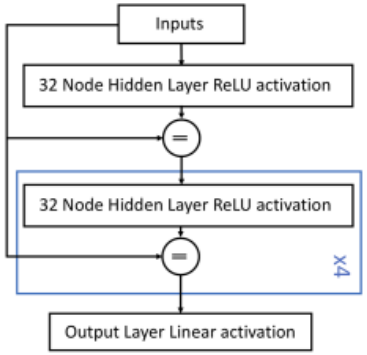

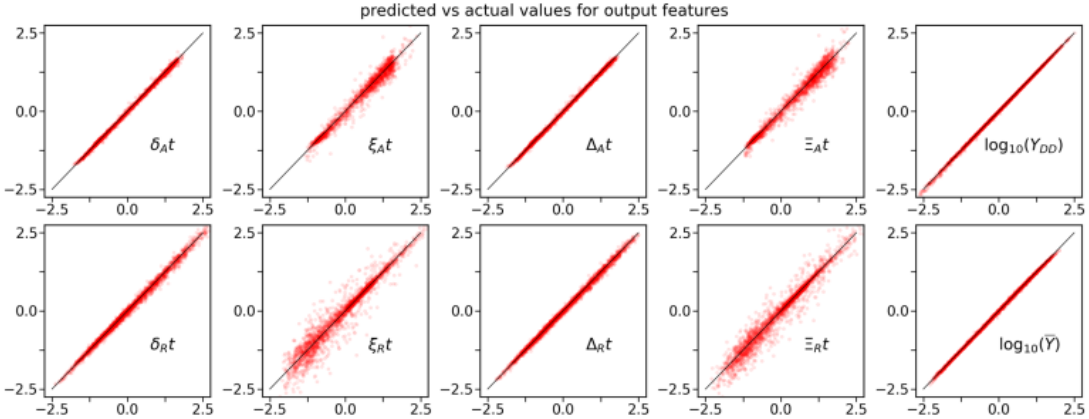

W.E. Lewis *et al.,* Phys. Plasmas **28**, 092701 (2021).

Our analysis is based on a Bayesian inference which makes use of NN surrogate for speedup of physics model.

Obtain secondary neutron Time of Flight (nToFs)

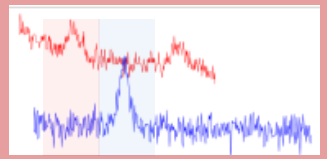

Select ROIs

Provide DT and DD yields with uncertainty

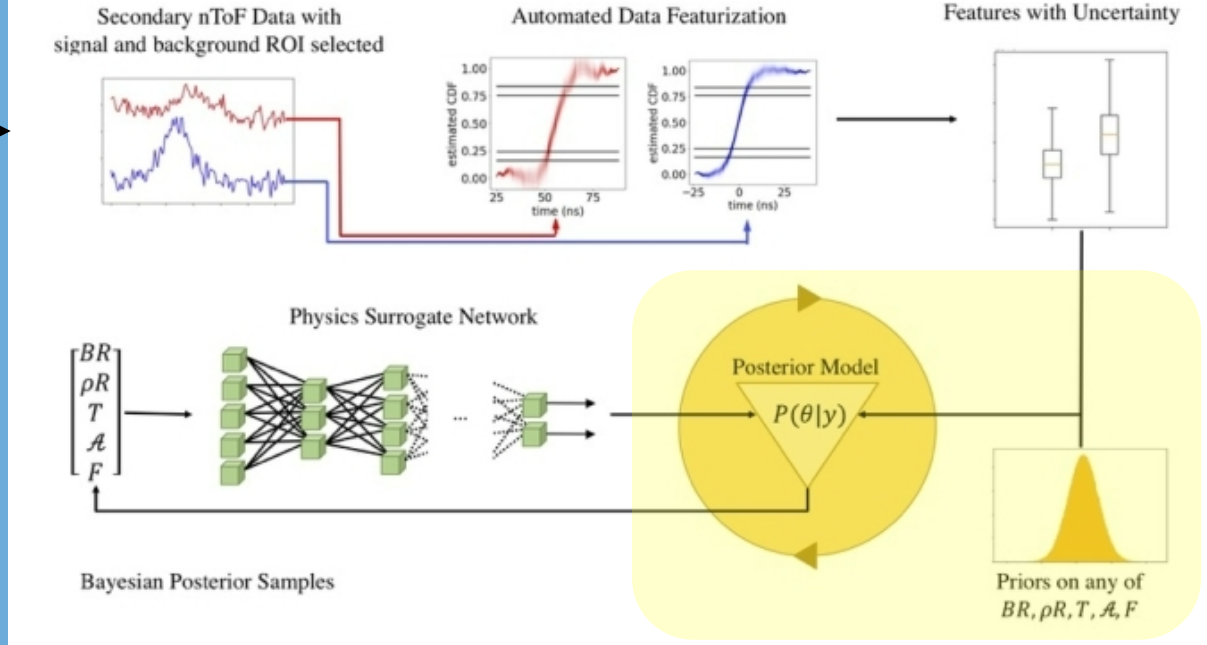

W.E. Lewis *et al.,* Phys. Plasmas **28**, 092701 (2021).

Bayes theorem allows us to incorporate multiple sources of data and rigorously define statistical data models for UQ.

- Sources of uncertainty considered:
  - Experimental data (multivariate normal)
  - Surrogate model (multivariate normal)

Bayes theorem allows us to incorporate multiple sources of data and rigorously define statistical data models for UQ.

- Sources of uncertainty considered:
  - Experimental data (multivariate normal)
  - Surrogate model (multivariate normal)

We can encode assumptions about statistics in Bayesian framework with a bit of maths.

A bit of maths… let's chat after or see 1 or 1 if interested in details

Bayes theorem and manipulations:

Posterior distribution for parameters (x) given data (y)

Prior information on parameters

$$p(\mathbf{x}|\mathbf{y}) = p(\mathbf{y}|\mathbf{x})p(\mathbf{x})/p(\mathbf{y})$$

Likelihood function describing distribution of data around model

Parameter independent normalization (unimportant)

Introduce latent variable z to track uncertainty from surrogate → $p(\mathbf{x}|\mathbf{y}) = \int p(\mathbf{x},\mathbf{z}|\mathbf{y})d\mathbf{z}$

Bayes theorem for data including surrogate model → $p(\mathbf{x},\mathbf{z}|\mathbf{y}) \propto p(\mathbf{y}|\mathbf{x},\mathbf{z})p(\mathbf{z}|\mathbf{x})p(\mathbf{x})$

Our data models:

Physics model value normally distributed about NN prediction with OOS estimate of covariance

$$p(\mathbf{z}|\mathbf{x}) \sim \mathcal{N}(f_{NN}(\mathbf{x}), \Lambda_{NN})$$

Assumed independence of different measured quantities

$$\begin{aligned} p(\mathbf{y}|\mathbf{x},\mathbf{z}) &= p(\mathbf{y}|\mathbf{z}) \\ &= p(\mathbf{y}_{\text{ntoF}}|\mathbf{z}_{\text{ntoF}})p(y_Y|z_Y)p(y_{\overline{Y}}|z_{\overline{Y}}) \end{aligned}$$

Observations normally distributed about "latent model"

$$p(y_Y|z_Y) \sim \mathcal{N}(z_Y, \Lambda_Y)$$

$$p(y_{\overline{Y}}|z_{\overline{Y}}) \sim \mathcal{N}(z_{\overline{Y}}, \Lambda_{\overline{Y}})$$

$$p(\mathbf{y}_{\text{nToF}}|\mathbf{z}_{\text{nToF}}) \sim \mathcal{N}(\mathbf{z}_{\text{nToF}}, \Lambda_{\text{nToF}})$$

A bit of maths… let's chat after or see 1 on 1 if interested in details

Advanced Data Analysis in Inertial Confinement Fusion and High Energy Density Physics

P. F. Knapp[1] and W. E. Lewis[1]
Sandia National Laboratories, Albuquerque, New Mexico 87185, USA

Tutorial on Bayesian inference with code

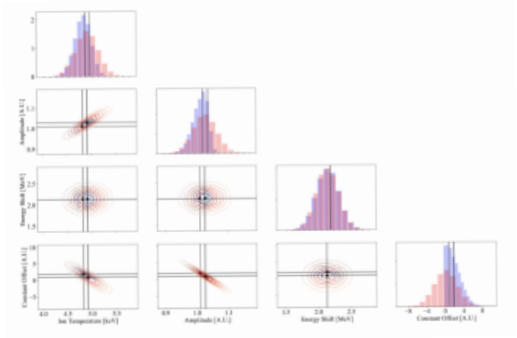

Extensive ICD/HEDP literature review of:

Bayesian inference

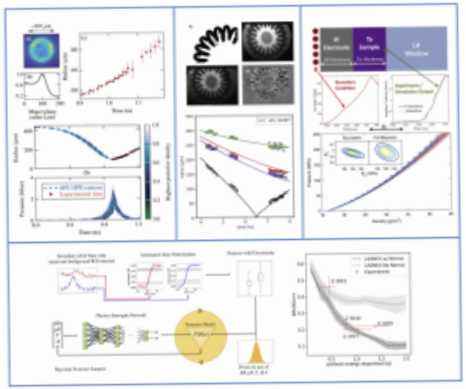

Applied ML methods

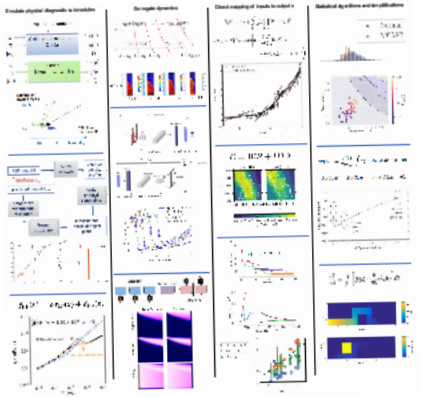

Submitted to special issue of Rev. Sci. Instrum.

Ba

Poste
parame

Lik
descr
da

Introd
z to
f

Bayes t
including surrogate model

ut
ce

uantities

t model"

$$p(\mathbf{y}_{\mathrm{nToF}}|\mathbf{z}_{\mathrm{nToF}}) \sim \mathcal{N}(\mathbf{z}_{\mathrm{nToF}}, \Lambda_{\mathrm{nToF}})$$

deposited in the fuel show a trend consistent with Nernst effect.

- Evaluated fast-particle confinement parameter
  - across family of experiments varying preheat energy
  - rigorously defined UQ
- Consistent with flux loss via Nernst.

Nernst effect
- B-field locked into warm electrons
- Thermal transport perpendicular to B transports flux

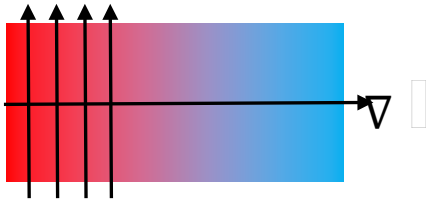

$$v_{Nernst} \sim \frac{\nabla_{\perp} T_e}{eB}$$

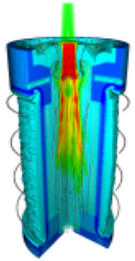

$AR = r_O/\Delta r$

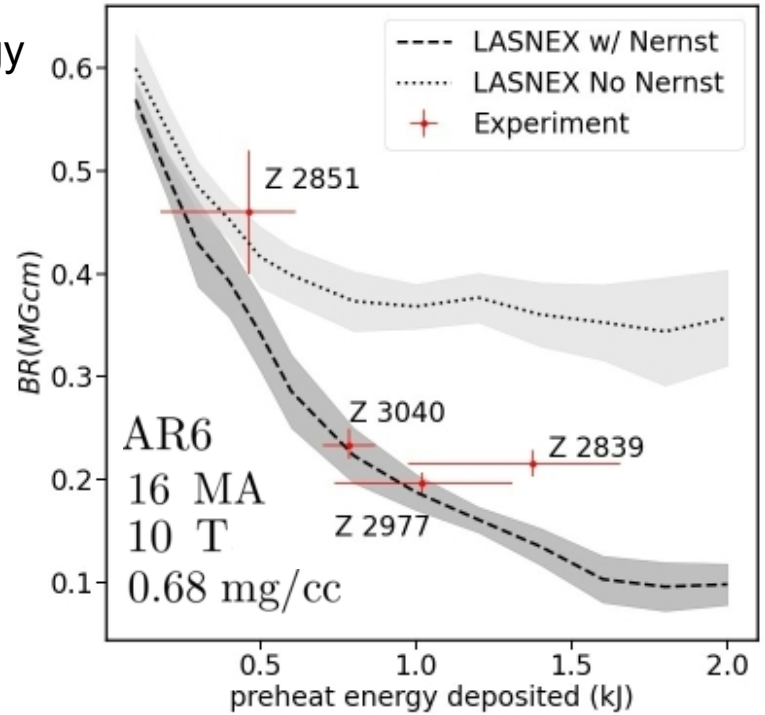

W.E. Lewis *et al.,* Phys. Plasmas **28**, 092701 (2021).

Nernst is integral to performance scaling in MagLIF.

- Nernst limits the gains by increasing preheat alone
  - ρ_{fill}, B_z, I_{max} *etc.* must be improved to enable performance gains

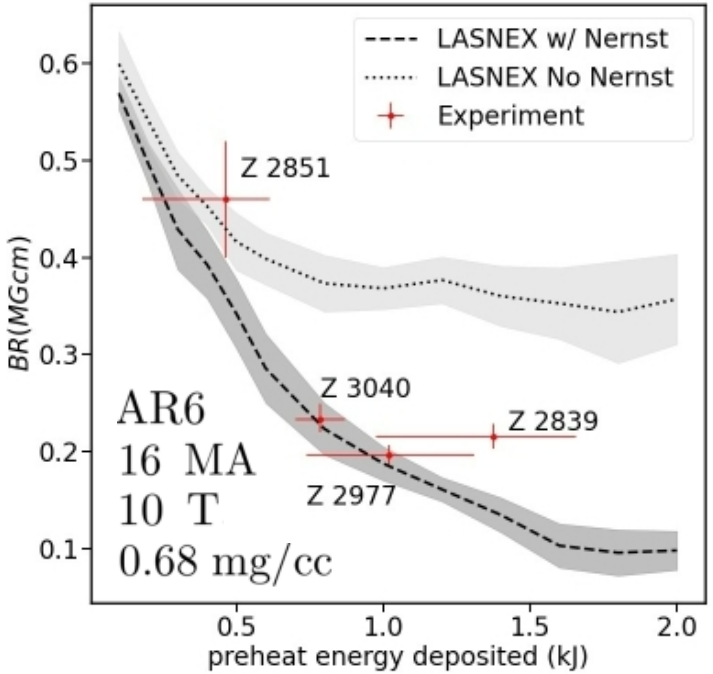

W.E. Lewis *et al.,* Phys. Plasmas **28**, 092701

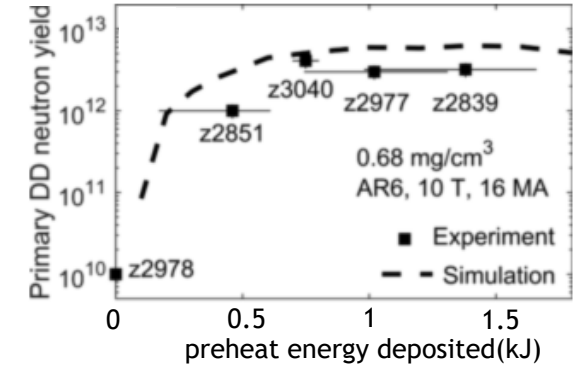

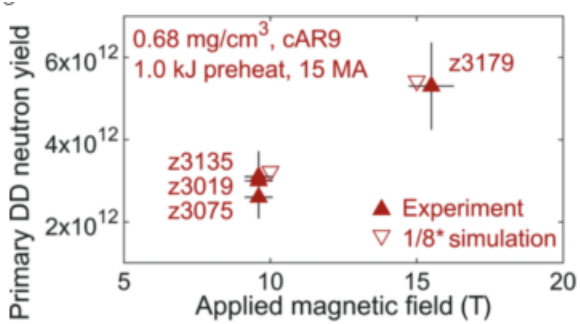

M.R. Gomez *et al.,* PRL **125**, 155002

We can use this tool to let our data tell us the larger story behind the physics of magnetic confinement in MagLIF

- **How do other experiment inputs impact flux loss?**
  - fill density/target height
  - aspect ratio
  - inner liner radius
  - mix
  - B_z
- Gray points reference cases PoP 2021:
  - $AR = 6, B_z = 10\ T$, and $\rho_{fill} = 0.7\ mg/cc$

$$AR = \frac{R_{0,out}}{R_{0,out} - R_{0,in}}$$

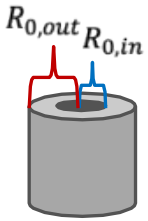

- 1D resistive radMHD code Kraken* for comparison
  - C.A. Jennings implementation of GORGON system of MHD equations

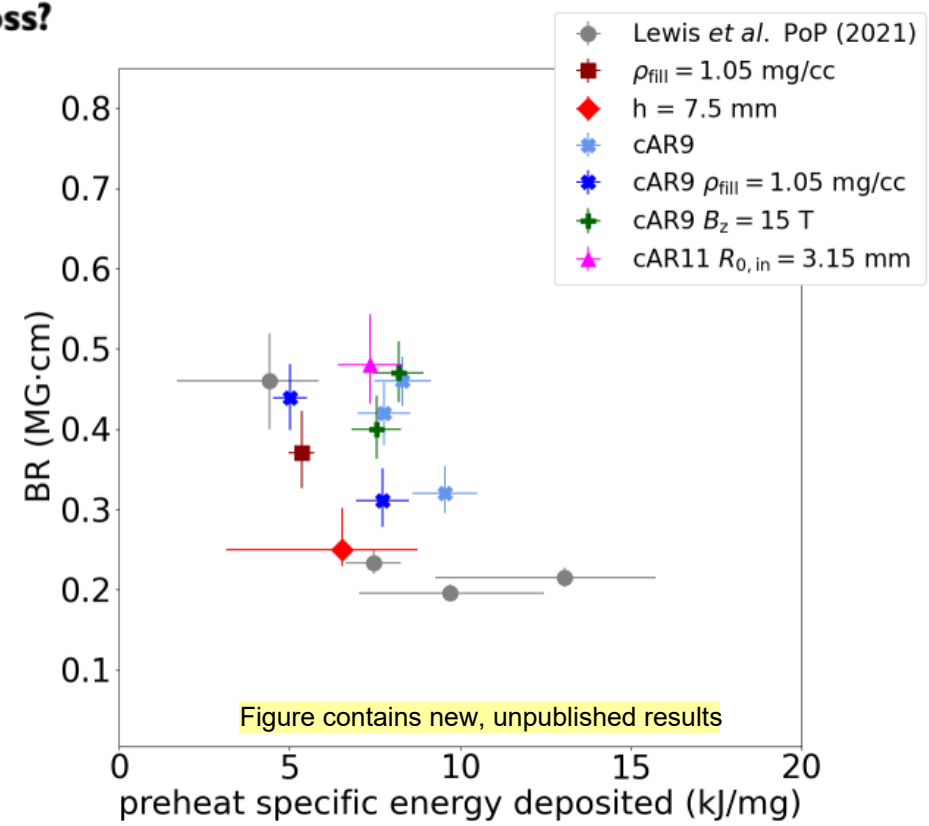

impact of Nernst vs PSE is nearly independent of fill density

- $T_{preheat}$ appears to dominate scaling
  - Flux loss relatively insensitive to
    - ρ_{fill}
    - target height
- Bands show $\rho_{fill} = 0.7 - 1.05$ mg/cc range

$$PSE = \frac{PE\ deposited}{fuel\ mass}$$

$$\langle T_{preheat} \rangle \propto PSE \qquad x_e \propto \frac{{T_e}^{3/2} B}{\rho} \sim B/\rho \text{ at fixed PSE}$$

$$v_{Nernst} = \frac{\beta_\wedge(x_e)\nabla_\perp T_e}{eB}$$

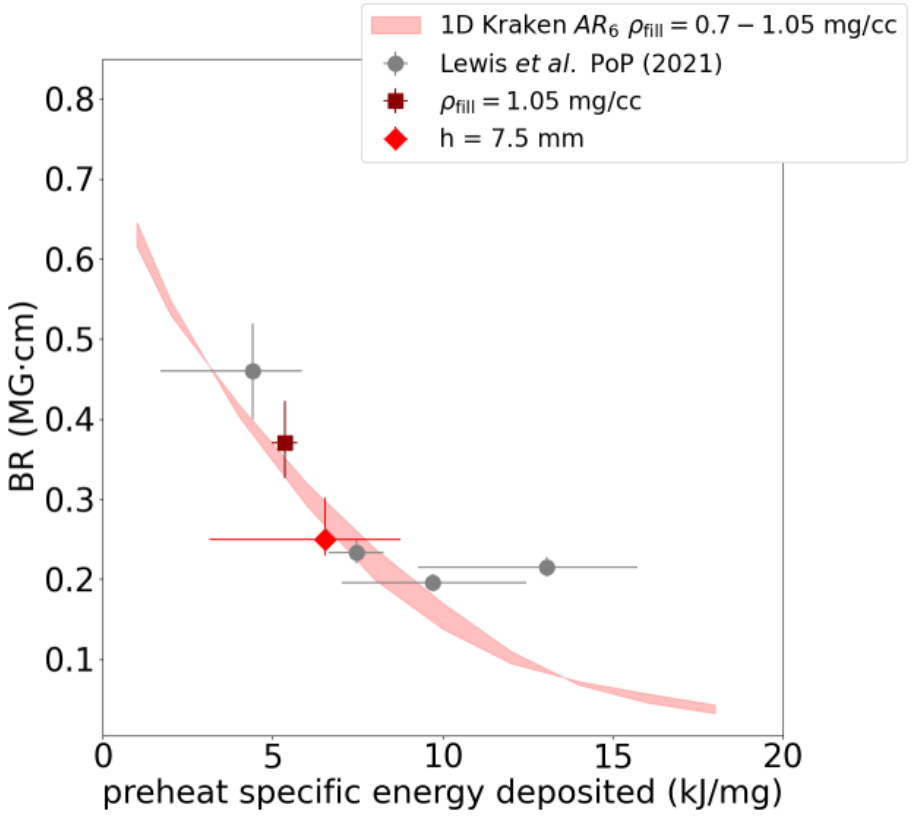

Increasing AR increases BR, largely through increased compression of fuel (CR) and hence magnetic flux

Increasing AR

- Less mass easier to compress

$$CR = \frac{R_{in,0}}{R_{in,f}} \qquad (BR)_f = CR\,\frac{\phi_f}{\phi_0}(BR)_0$$

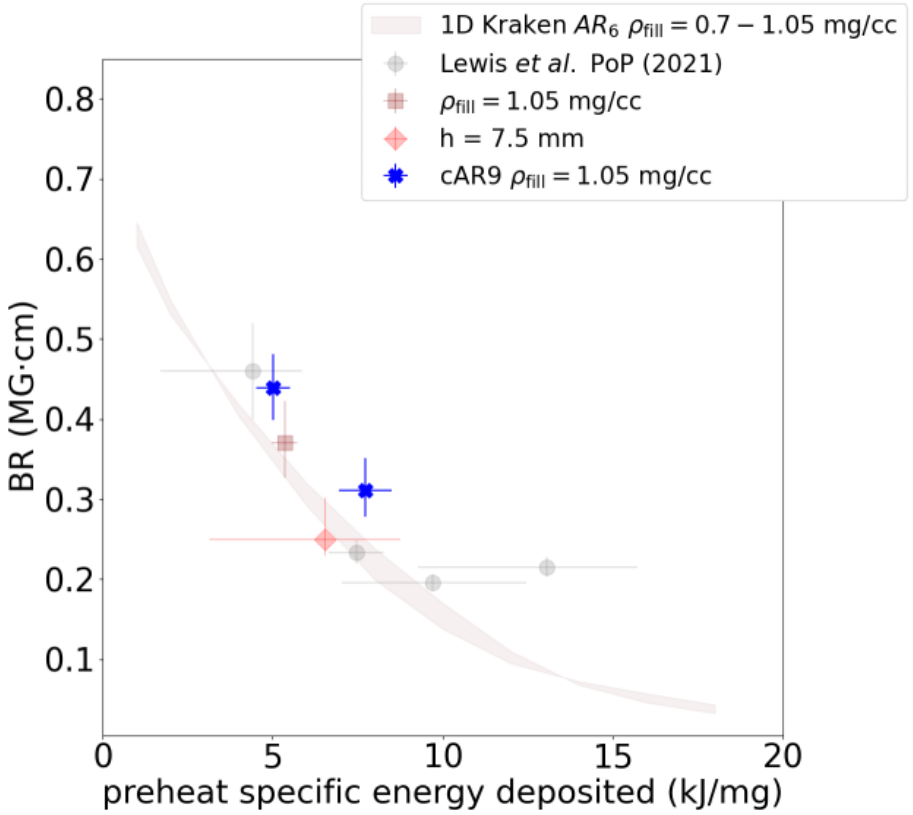

Increasing AR increases BR, largely through increased compression of fuel (CR) and hence magnetic flux

Increasing AR

- Less mass easier to compress

$$CR = \frac{R_{in,0}}{R_{in,f}} \qquad (BR)_f = CR\,\frac{\phi_f}{\phi_0}(BR)_0$$

- Simulations show
  - 20-30% higher CR
  - CR impact dominant over flux loss

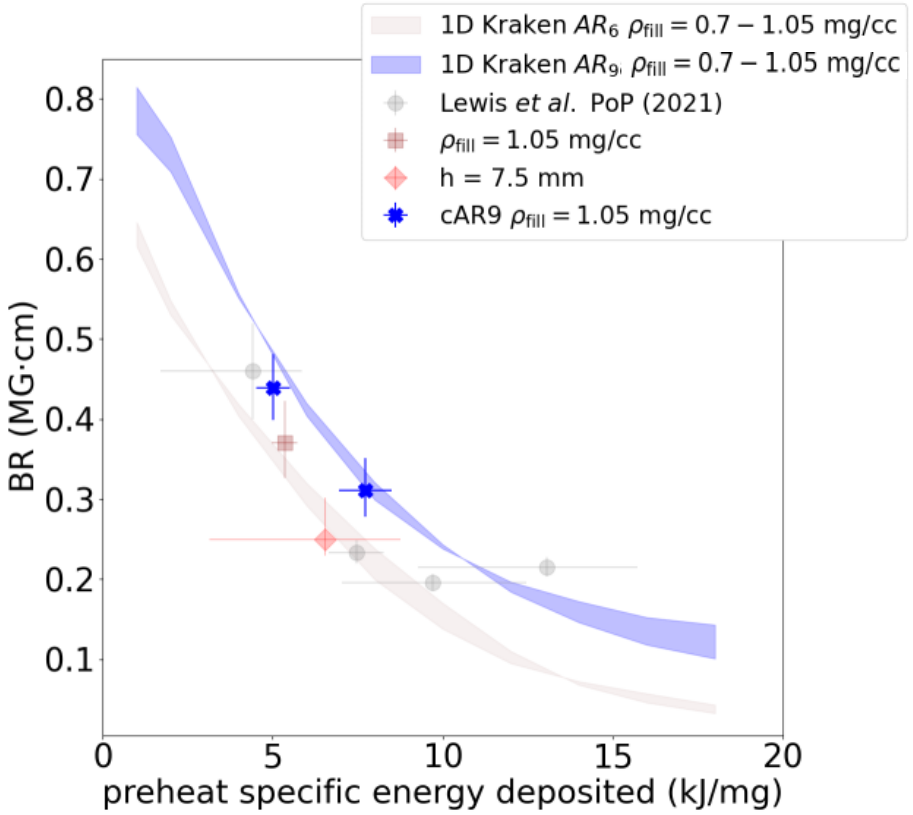

through $(BR)_0$ while CR and total flux loss effects depend on details

Increasing AR and $R_{in,0}$

- $(BR)_0$ increases with $R_{in,0}$
  - 35% larger for AR11 target

$$CR = \frac{R_{in,0}}{R_{in,f}} \qquad (BR)_f = CR\,\frac{\phi_f}{\phi_0}(BR)_0$$

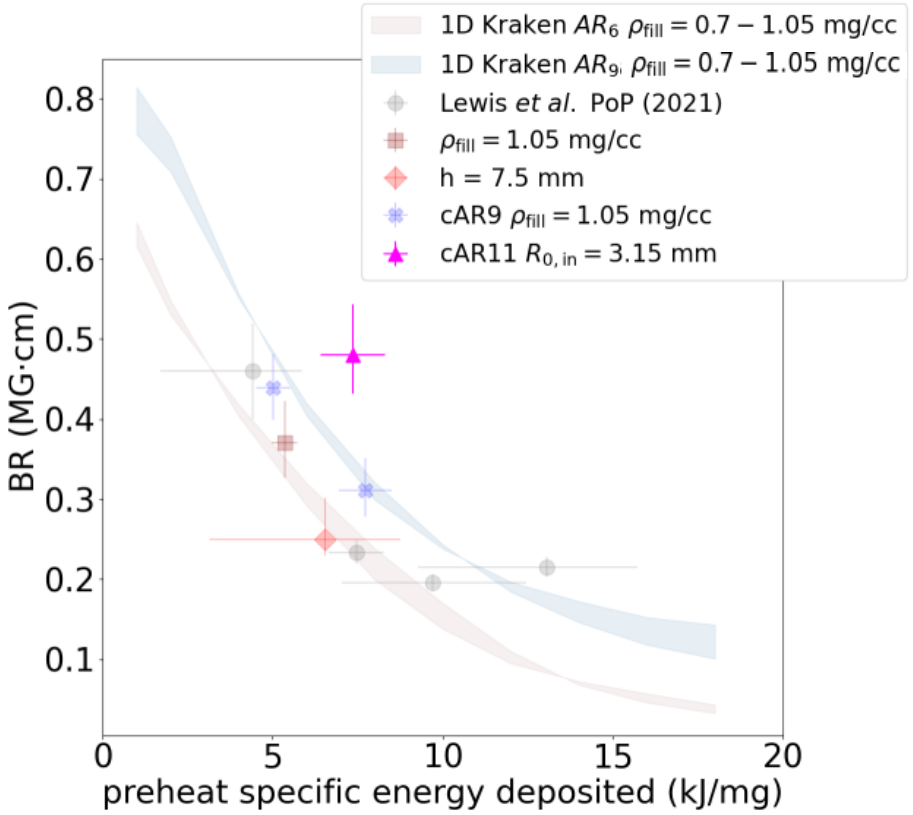

through $(BR)_0$ while CR and total flux loss effects depend on details

Increasing AR and $R_{in,0}$

- $(BR)_0$ increases with $R_{in,0}$
  - 35% larger for AR11 target

$$CR = \frac{R_{in,0}}{R_{in,f}} \qquad (BR)_f = CR\frac{\phi_f}{\phi_0}(BR)_0$$

- Simulation shows
  - Similar CR to AR6 target
    - ~35% increase to BR over AR6
    - ~10-20% increase over AR9

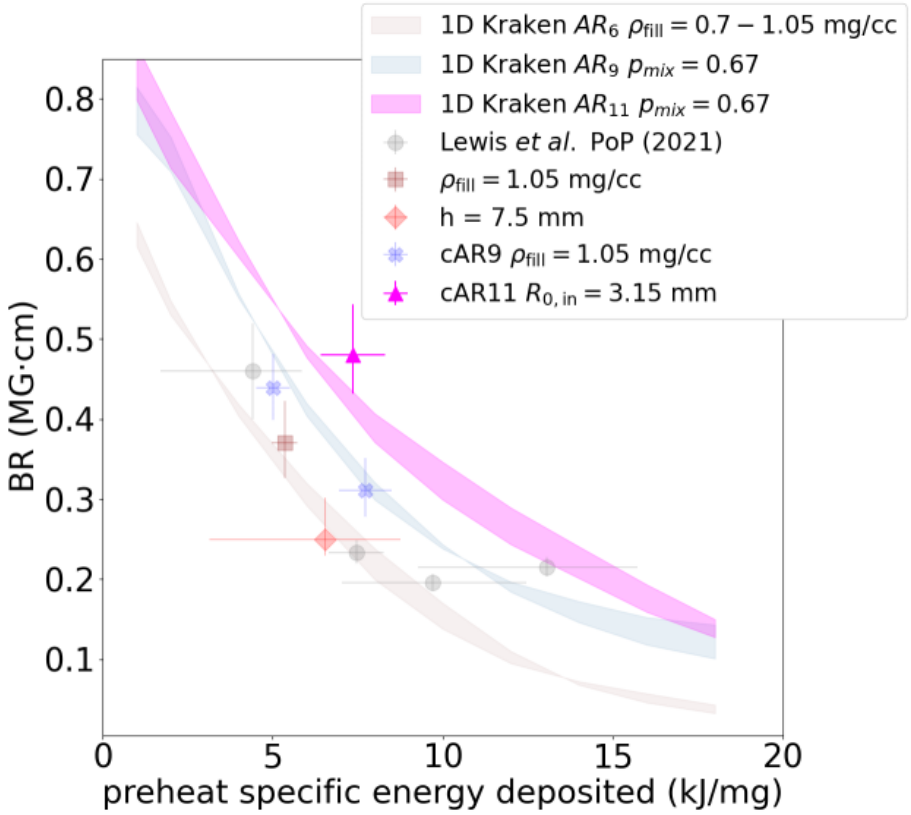

Lower fill density cAR9 shots show anomalously high BR which may be a result of introducing significant mix*

- Mix enhances radiative losses
  - Can cool the fuel leading to
    - Reduced temperature gradients
    - Higher CR
    - Reduced performance

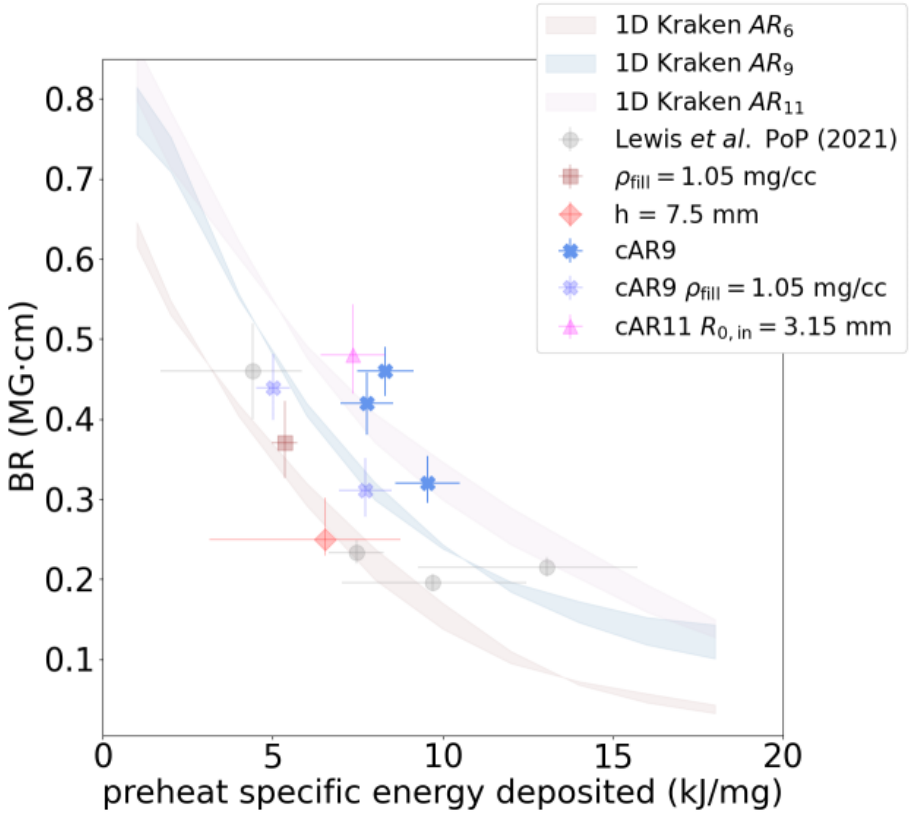

*Ratio of x-ray to DD neutron yield is consistent with the increased mix interpretation

Lower fill density cAR9 shots show anomalously high BR which may be a result of introducing significant mix*

- Mix enhances radiative losses
  - Can cool the fuel leading to
    - Reduced temperature gradients
    - Higher CR
    - Reduced performance
- Results appear consistent with
  - 1D simulations
  - Y_v / Y_{DD}
  - Bayesian inference of mix

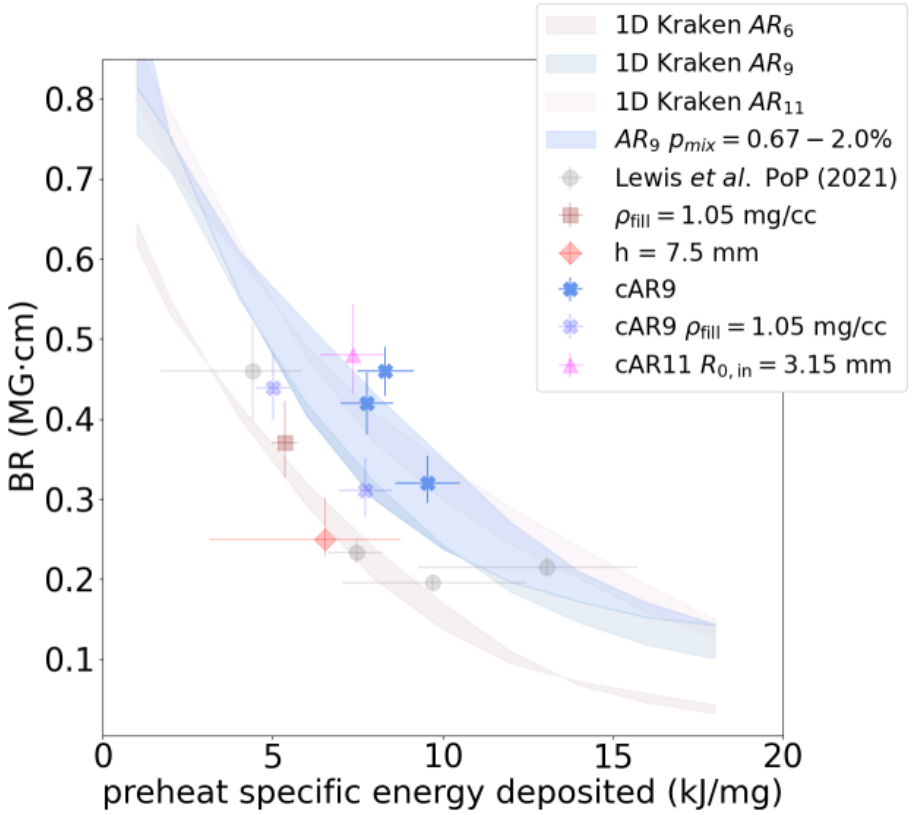

*Ratio of x-ray to DD neutron yield is consistent with the increased mix interpretation

Increasing Bz is expected to increase BR through $(BR)_0$ but flux loss and CR depend on details

- $(BR)_0$ increases with B_z (50% larger)

$$(BR)_f = CR\frac{\phi_f}{\phi_0}(BR)_0$$

- Reduced thermal conduction
  - Possibly changes to temperature gradients
  - May reduce CR

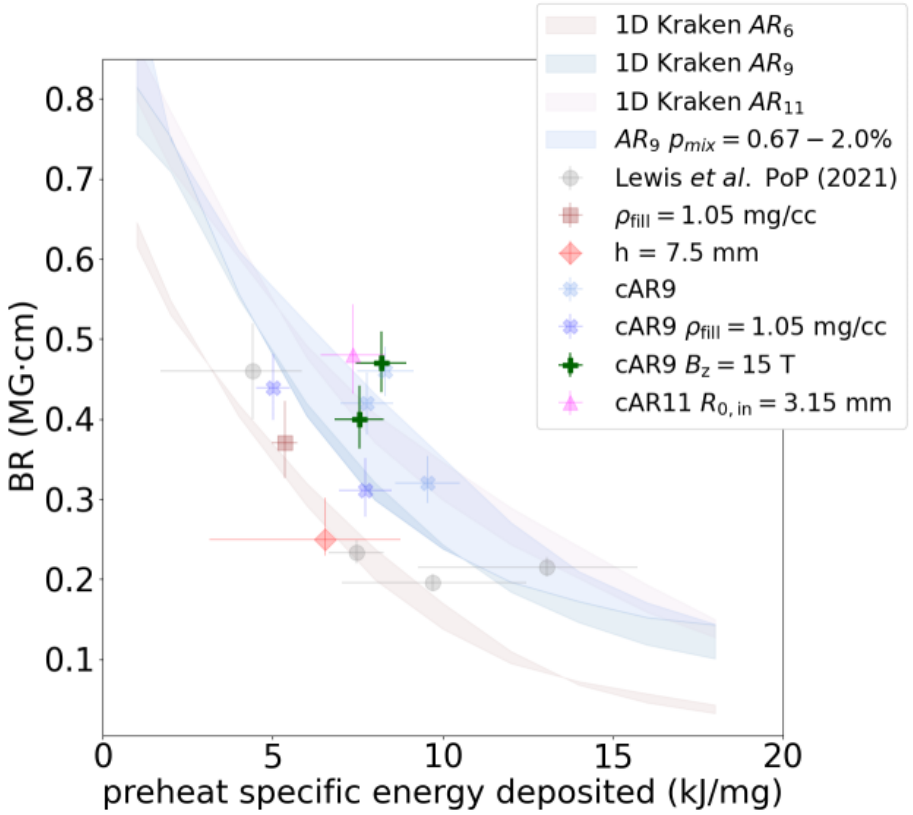

Increasing Bz is expected to increase BR through $(BR)_0$ but flux loss and CR depend on details

- $(BR)_0$ increases with B_z (50% larger)

$$(BR)_f = CR\,\frac{\phi_f}{\phi_0}(BR)_0$$

- Reduced thermal conduction
  - Possibly changes to temperature gradients
  - May reduce CR
- Simulation shows
  - ~50% increase to BR over AR9 10T
  - Initial field effect seems dominant
- Laser alignment issue → 3D effects?

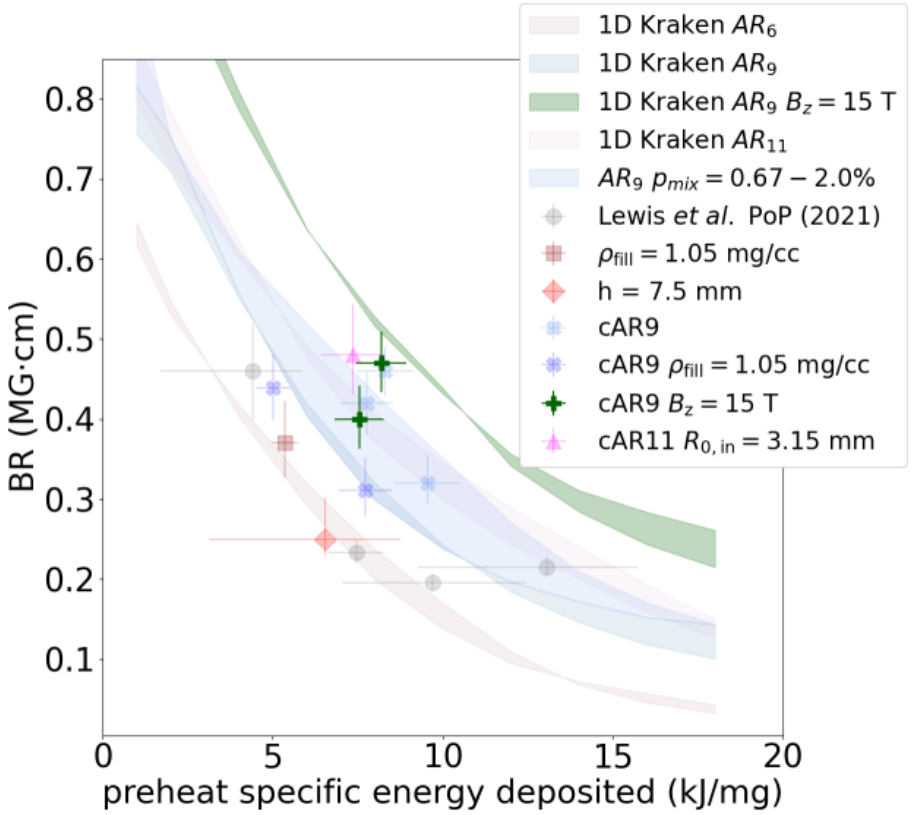

Our model makes simplifying assumptions pointing to interesting open questions, but well reproduced observations encourage its application.

- nToF shape features
- 2 ns Gaussian burn history
- $T_e = T_i$
- 1D power law profile model with
  - $B_z \propto \rho$
  - Axially uniform B-field
- **Unknown impact of 3D effects**

Magnetic field topology alters secondary neutron spectra

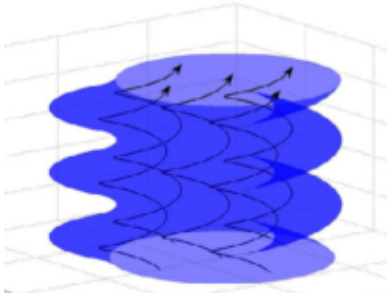

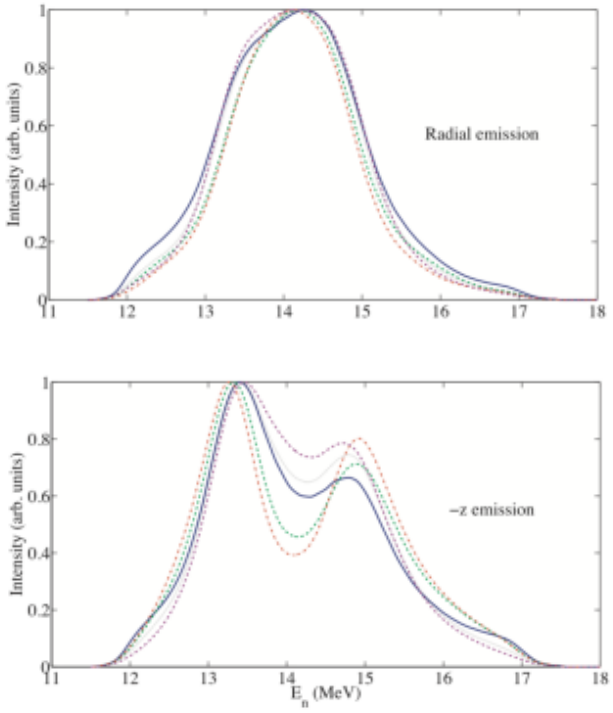

B. Appelbe *et al.*, HEDP **22**, 27 (2017).

simulations that may enable us to better characterize the importance of 3D effects.

Statistical characterization of experimental magnetized liner inertial fusion stagnation images using deep-learning-based fuel–background segmentation

- Tool to process images

- Characterized noise and background
  - Can be used for UQ

W.E. Lewis *et al.,* J. Plasma Phys. **88**, 895880501 (2022).

- Investigate impact of 3D on BR
  - 3D simulation studies*
  - Image analysis tools

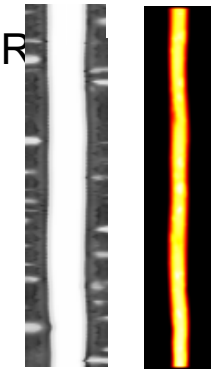

*Animations courtesy C.A. Jennings

Invited talk at ICDDPS-4 (Okinawa, JP) 4/22

A framework for experimental-data-driven assessment of Magnetized Liner Inertial Fusion stagnation image metrics*

- Framework to understand sensitivity
  - SNR, resolution, registration, *etc.*
- Metrics for image-to-image comparison

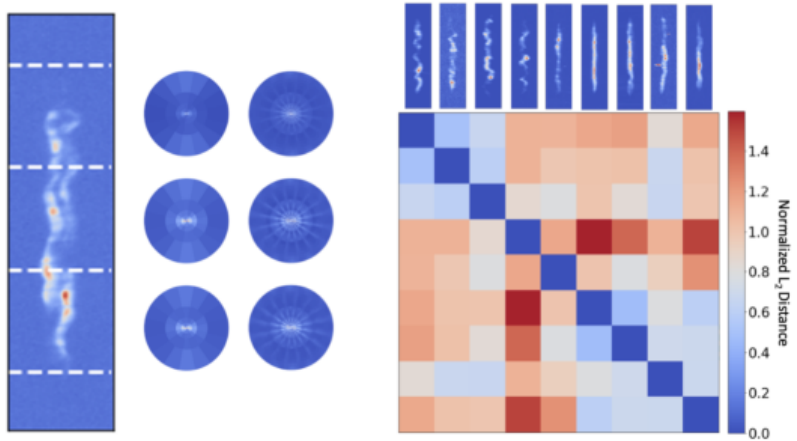

W.E. Lewis *et al.,* In Preparation.

Closing remarks

Method + initial analysis:

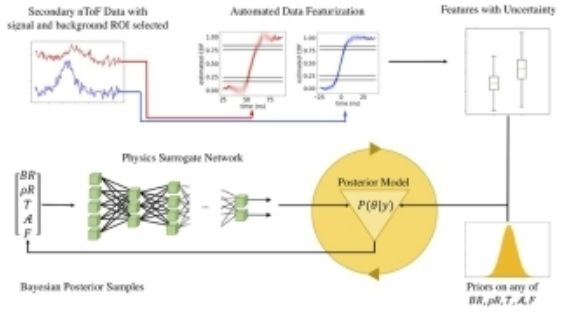

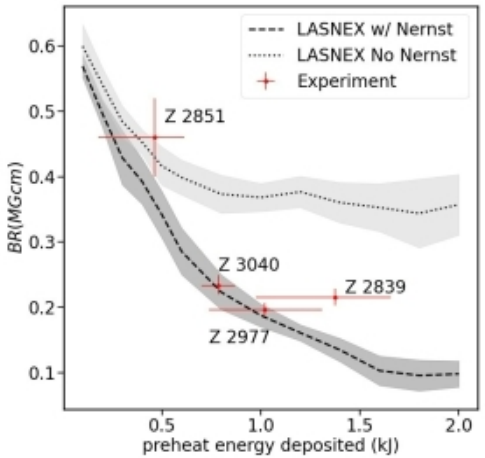

W.E. Lewis *et al.,* Phys. Plasmas **28**, 092701 (2021).

New analysis:

- Scaling of BR/flux compression
  - Fill density, AR, $R_{in,0}$, mix, B_z

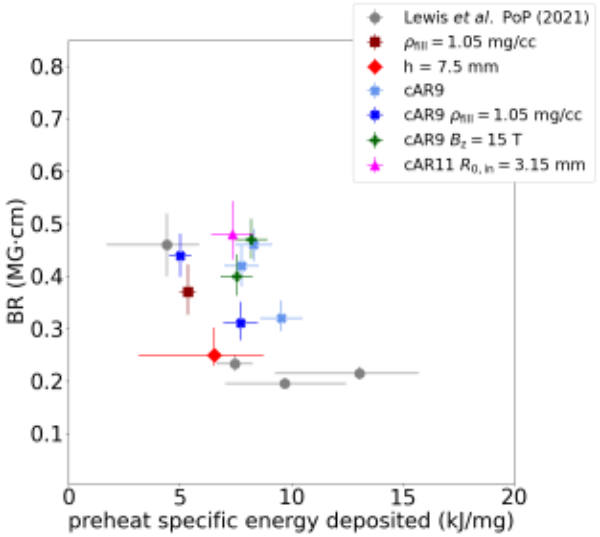

W.E. Lewis *et al.,* In Preparation.

Future directions:

interested in collaborations!

- Next generation pulsed power
- 3D effects
- Relaxed assumptions
- Current scaling

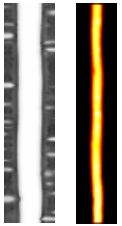

C.A. Jennings

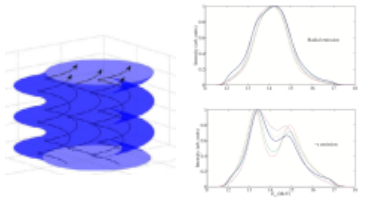

B. Appelbe *et al.,* HEDP **22**, 27 (2017).

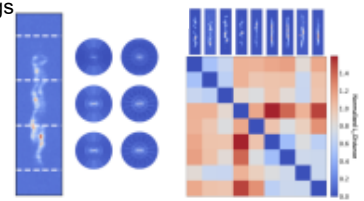

W.E. Lewis *et al.,* In Preparation.

Backup Slides

synthetic datasets and the only available previously analyzed experiment.

- Surrogate model quantitatively captures features of physics model
- We have demonstrated that BR inference on noisy synthetic data is robust to S/N ratios comparable to experiment
- Results are consistent with the only available previously analyzed experiment.

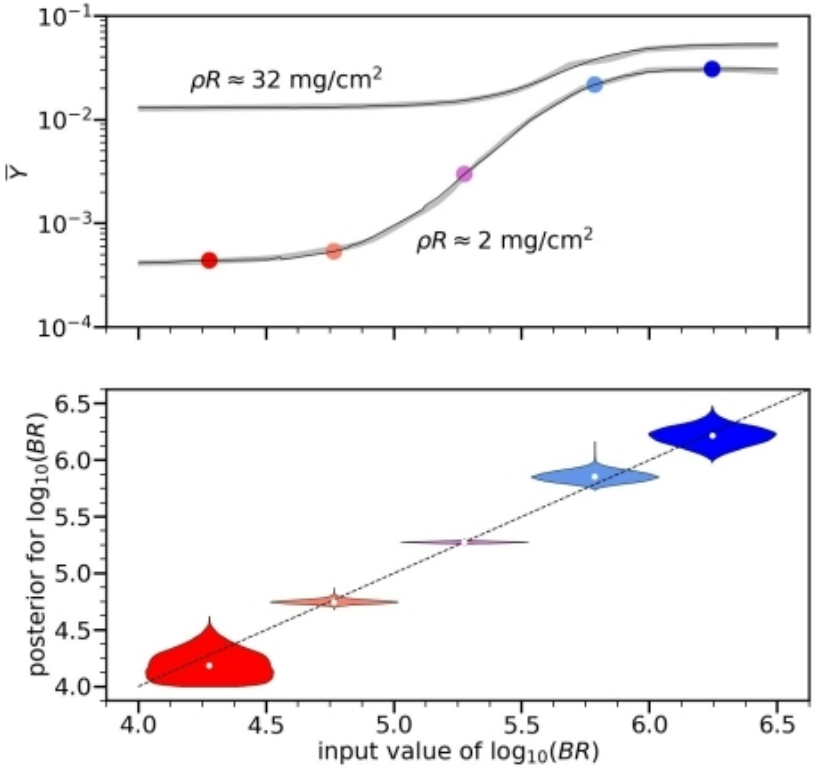

W.E. Lewis *et al.*, accepted Phys. Plasmas (2021).

synthetic datasets and the only available previously analyzed experiment.

Shape features, DD and DT yields sufficient for BR recovery from noisy synthetic data even when other model parameters obscured.

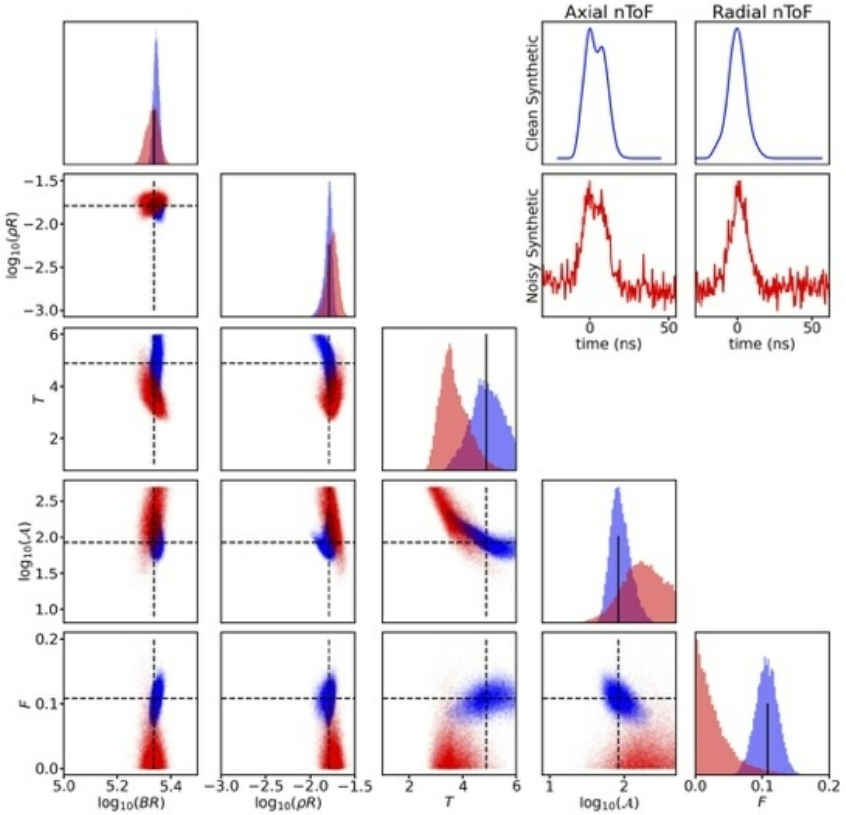

W.E. Lewis *et al.*, accepted Phys. Plasmas (2021).

synthetic datasets and the only available previously analyzed experiment.

Results are consistent with previous analysis of z2591

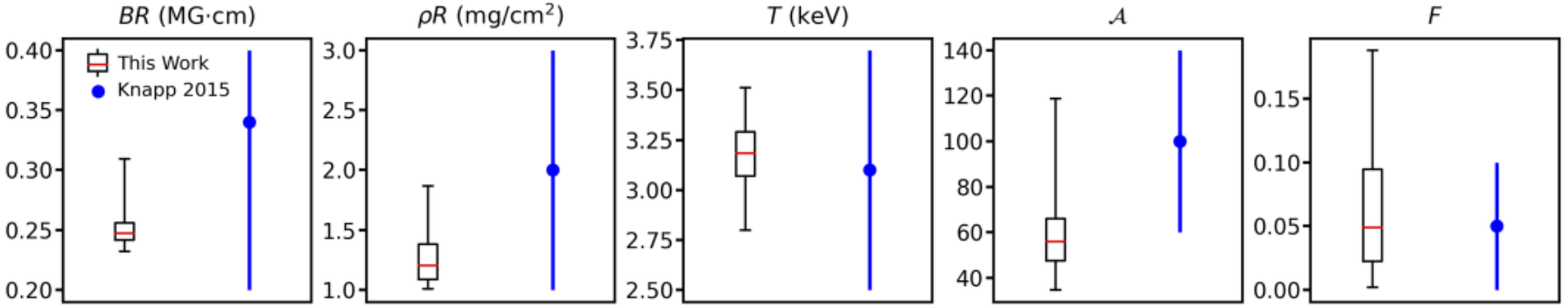

W.E. Lewis *et al.*, accepted Phys. Plasmas (2021).

physics model, good agreement with observations is obtained.

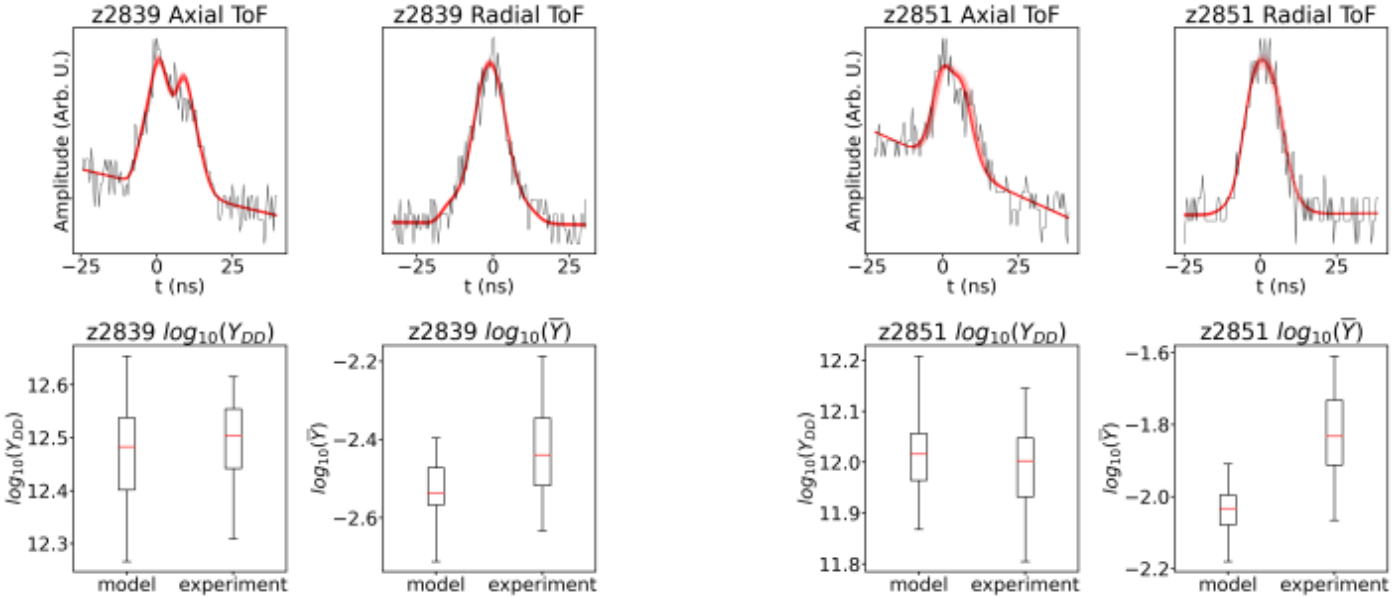

The agreement obtained with observations indicates that our results are consistent with what would be obtained were it feasible to conduct a Bayesian analysis using the full physics model.

Bayes theorem allows us to incorporate multiple sources of data and rigorously define statistical data models for UQ.

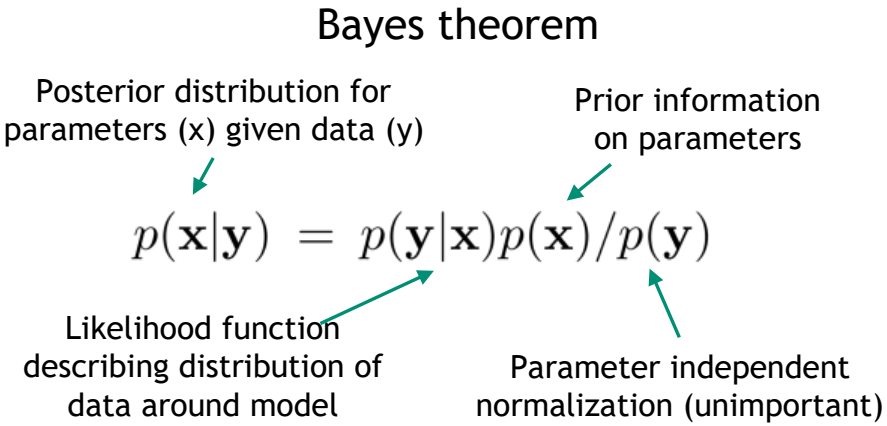

- Provides a distribution of model parameters most consistent with data
- We incorporate sources of uncertainty from:
  - use of NN surrogate
  - featurizing nToF
  - DD and DT yield measurements

X-ray to DD yield ratios are consistent with higher mix for the lower fill density coated AR9 experiments analyzed for BR

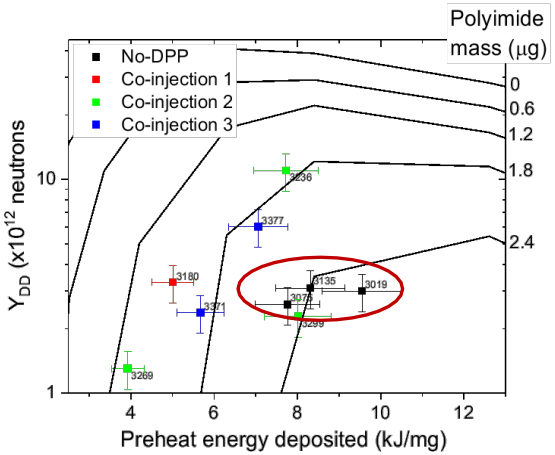

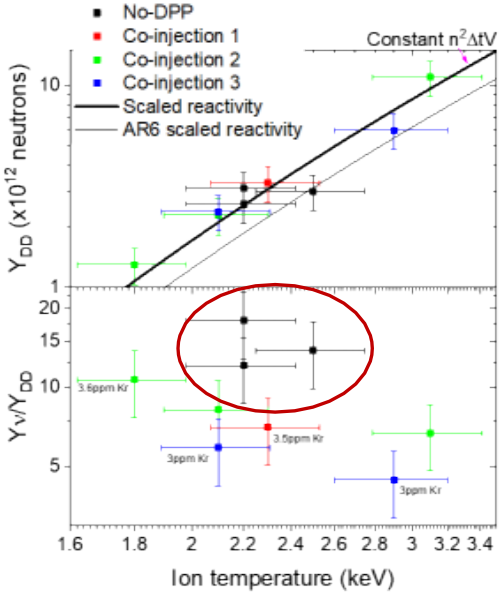

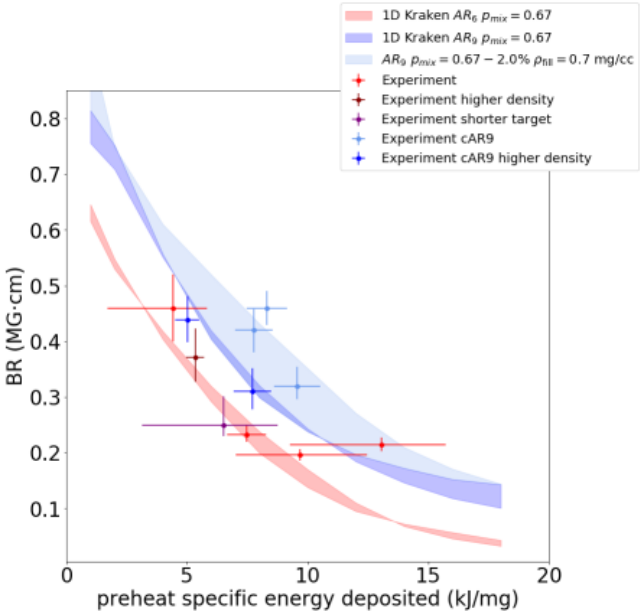

A.J Harvey-Thompson *et al.* In Preparation.

$$P_\nu = A_{ff} 4\pi P_{HS}^2 e^{-\tau_\nu^\ell} \int_{V_{HS}} \frac{\langle Z \rangle g_{FF}}{(1+\langle Z \rangle)^2} \sum_i f_i \tilde{j}_i \frac{e^{-h\nu/T_e}}{T_e^{5/2}} dV$$

$$Y_{DD} = \frac{1}{2} P_{HS}^2 \tau_b \int_{V_{HS}} \frac{\langle \sigma v \rangle_{DD}}{(1+\langle Z \rangle)^2 T_i^2} dV$$

P.F. Knapp *et al.* Phys. Plasmas **26**, 012704 (2019).